Journal of Virology

Persistent Infection of Thymic Epithelial Cells with Coxsackievirus B4 Results in Decreased Expression of Type 2 Insulin-Like Growth Factor

Hela Jaïdane, Delphine Caloone, Pierre-Emmanuel Lobert, Famara Sane, Olivier Dardenne, Philippe Naquet, Jawhar Gharbi, Mahjoub Aouni, Vincent Geenen and Didier Hober
J. Virol. **2012, 86(20):11151. DOI: 10.1128/JVI.00726-12. Published Ahead of Print 1 August 2012.**

JVI Journals.ASM.org

Persistent Infection of Thymic Epithelial Cells with Coxsackievirus B4 Results in Decreased Expression of Type 2 Insulin-Like Growth Factor

Hela Jaïdane,[a,b,c] Delphine Caloone,[a] Pierre-Emmanuel Lobert,[a] Famara Sane,[a] Olivier Dardenne,[d] Philippe Naquet,[e] Jawhar Gharbi,[b] Mahjoub Aouni,[b] Vincent Geenen,[d] and Didier Hober[a]

Université Lille 2, Faculté de Médecine, CHRU, Laboratoire de Virologie/EA3610, Loos-lez-Lille, France[a]; Université de Monastir, Laboratoire des Maladies Transmissibles et Substances Biologiquement Actives LR99ES27, Faculté de Pharmacie de Monastir, Monastir, Tunisia[b]; Université de Tunis el Manar, Faculté des Sciences de Tunis, Tunis, Tunisia[c]; University of Liege, GIGA Research—Center of Immunology, CHU-B34, Liege-Sart Tilman, Belgium[d]; and Centre d'Immunologie INSERM-CNRS de Marseille-Luminy, Marseille, France[e]

It has been hypothesized that a disturbance of central self-tolerance to islet β cells may play a role in the enteroviral pathogenesis of type 1 diabetes. Whether enteroviruses can induce an impaired expression of β-cell self-antigens in thymic epithelial cells has been investigated in a murine thymic epithelial (MTE) cell line. This cell line was permissive to the diabetogenic group B4 coxsackievirus (CV-B4) strain CV-B4 E2 and spontaneously expressed type 2 insulin-like growth factor (Igf2), the dominant self-antigen of the insulin family. In this model, a persistent replication of CV-B4 E2 was obtained, as attested to by the prolonged detection of intracellular positive- and negative-strand viral RNA by reverse transcription-PCR (RT-PCR) and capsid protein VP1 by immunofluorescent staining and by the release of infectious particles in culture supernatants. The chronic stage of the infection was characterized by a low proportion of VP1-positive cells (1 to 2%), whereas many cells harbored enteroviral RNA, as displayed by RT-PCR without extraction applied directly to a few cells. *Igf2* mRNA and IGF-2 protein were dramatically decreased in CV-B4 E2-infected MTE cell cultures compared with mock-infected cultures, whereas housekeeping and interleukin-6 (*Il6*) gene expression was maintained and *Igf1* mRNA was decreased, but to a lower extent. Inoculation of CV-B3, CV-B4 JVB, or echovirus 1 resulted in a low level of IGF-2 in culture supernatants as well, whereas herpes simplex virus 1 stimulated the production of the protein. Thus, a persistent infection of a thymic epithelial cell line with enteroviruses like CV-B4 E2 can result in a disturbed production of IGF-2, a protein involved in central self-tolerance toward islet β cells.

Members of the group B coxsackieviruses (CV-Bs), belonging to the *Enterovirus* genus of the *Picornaviridae* family, are small, nonenveloped, single-strand positive RNA viruses. Numerous epidemiological studies associated CV-B infections with the onset of type 1 diabetes (T1D), giving evidence of their possible involvement as triggering agents of that disease in genetically predisposed individuals (reviewed in references 24, 30, and 62). CV-B4 is one of the serotypes most frequently encountered in diabetic patients (10, 15, 44, 46, 47, 63, 65; reviewed in reference 28).

T1D results from the autoimmune destruction of pancreatic insulin-producing islet β cells. Autoimmunity is the consequence of self-tolerance failure at the central and/or the peripheral level (56). Self-tolerance establishment is initiated within the thymus network during T-cell ontogeny by deletion of autoreactive T lymphocytes (negative selection) and generation of regulatory T cells (31, 51, 54). Elimination of potentially self-reactive T cells in the thymus requires the intrathymic expression of ubiquitous and tissue-specific antigens (38). This phenomenon has been termed "promiscuous" gene expression and appeared to be a unique property of medullar thymic epithelial cells (TECs) (38). Thus, the majority of self-antigens are expressed within the thymic microenvironment (1). It is also the case for the whole insulin family, since transcripts of insulin-like growth factor 2 (*Igf2*), *Igf1*, and insulin (*Ins*) genes have been characterized in human, rat, and mouse thymuses (21, 22, 33, 34, 61). At the peptide level, IGF-2 was shown to be the dominant polypeptide of the insulin family in the thymus epithelial network from different species (17, 18, 34).

An association between a defect in *Igf2* expression in the thymus and the emergence of autoimmune diabetes in biobreeding diabetes-prone (BBDP) rats was suggested. Indeed, this defect could contribute both to the impaired T-cell development and to the absence of central T-cell self-tolerance to the whole insulin hormone family (32).

Besides, *Igf2* could be employed both in the reprogramming of immunological tolerance to islet β cells and in the regeneration of a functional β-cell mass (20). On the basis of the close homology and cross-tolerance between insulin and IGF-2, a novel type of negative/tolerogenic self-vaccination is currently developed for prevention and cure of T1D (23). Indeed, administration of IGF-2-derived self-antigens (B11-25 sequence) to peripheral blood mononuclear cells from $DQ8^+$ type 1 diabetic patients seems to be an efficient approach in T1D prevention, since it elicits a tolerogenic/regulatory cytokine profile (interleukin-10 [IL-10], IL-10/gamma interferon [IFN-γ], and IL-4) statistically different from the one induced by Ins B9-23 (19). This issue is currently investigated by vaccination of NOD mice with recombinant human IGF-2 alone or in combination with adjuvants (20). The association between CV-B4 infection and the loss of immune self-tolerance is still unclear. We hypothesized that CV-B4 infection of the thymus could disturb the physiological function of that organ (reviewed in reference 29). It has been shown that CV-B4 infec-

Received 23 March 2012 **Accepted** 26 July 2012
Published ahead of print 1 August 2012
Address correspondence to Didier Hober, didier.hober@chru-lille.fr.

doi:10.1128/JVI.00726-12

tion of the thymus leads to abnormal T-lymphocyte maturation *in vivo* during the course of systemic infection of mice (8), *ex vivo* in murine fetal thymus organ cultures (7), and *in vitro* in cultured human fetal thymus fragments (6). Besides, with the key role of TECs in both T-cell development and the induction of central self-tolerance being well established (2, 3), we previously investigated the possible infection of those cells by CV-B4, and we demonstrated that CV-B4 can persistently infect primary cultures of human TECs and modulate the profile of cytokine secretion by these cells (5).

Primary TECs are difficult to obtain and to maintain in culture for long periods and, moreover, are heterogeneous (since TECs are derived from both the thymic cortex and medulla). Since the thymus fulfills its functions mainly during fetal and neonatal life, we decided to perform studies with tissues or cells derived from individuals at these stages of life. For this purpose, we took advantage of the availability of a murine medullar thymic epithelial (MTE) cell line derived from neonatal mice, MTE4-14 (42), to investigate the infection of that cell type with the CV-B4 E2 diabetogenic strain and to address the issue of *Igf2* expression in that system.

MATERIALS AND METHODS

Cells. The murine thymic epithelial cell line MTE4-14 is derived from C3H/J (*H-2*^{k}) thymic neonatal lobes and is of medullar origin (42). MTE cells were grown in Dulbecco's modified Eagle medium (DMEM; Gibco BRL) containing 4.5 g/liter glucose and sodium pyruvate and supplemented with 10% heat-inactivated fetal calf serum (FCS; Sigma), 1% L-glutamine (Gibco BRL), 50 μg/ml streptomycin, 50 IU/ml penicillin (BioWhittaker) and 0.2% epidermal growth factor (EGF; Sigma).

SK-N-AS is a human neuroblastoma epithelial cell line (57). The SK-N-AS cell line (kindly provided by N. Von Roy, Ghent University, Ghent, Belgium) was originally maintained in RPMI (Eurobio) supplemented with 10% heat-inactivated FCS, 1% L-glutamine, 50 μg/ml streptomycin, and 50 IU/ml penicillin. In order to produce IGF-2, SK-N-AS cells were transferred in serum-free N2E medium (DMEM, Ham's F-12 medium [50:50, vol/vol; Sigma] with 1.2 mg/ml sodium bicarbonate and 15 mM HEPES, 1 μg/ml transferrin, 30 nM selenium, 20 nM progesterone, 100 μM putrescine [Sigma], 50 U/ml penicillin, 50 μg/ml streptomycin, and 2 mM L-glutamine) supplemented with 1 μg/ml insulin. After several passages, insulin was omitted from the medium and the cells were continuously propagated in mitogen-free N2E medium. Human fibronectin (5 μg/ml; Sigma) was added to the medium at the time of plating. Medium used for feeding the cultures did not contain fibronectin.

Viruses. CV-B3 Nancy (American Type Culture Collection [ATCC], Manassas, VA), the diabetogenic strain CV-B4 E2 (kindly provided by J. W. Yoon, Julia McFarlane Diabetes Research Centre, Calgary, Alberta, Canada), the prototype CV-B4 JVB (kindly provided by J. Almond, Aventis Pasteur, Marcy l'Etoile, France), the echovirus 1 (E-1) Farouk strain (AFSSA, France), vesicular stomatitis virus (VSV; kindly provided by P. Lebon, Paris), herpes simplex virus 1 (HSV-1) HF strain (ATCC), and the encephalomyocarditis virus (EMCV) EMC strain (ATCC) were propagated in Vero cells (BioWhittaker) in Eagle's minimal essential medium (MEM; Gibco BRL) supplemented with 10% FCS, 1% L-glutamine, 50 μg/ml streptomycin, and 50 IU/ml penicillin. Supernatants were collected 3 days after inoculation, clarified by centrifugation at 2,000 × *g* for 10 min, divided into aliquots, and stored at −80°C. Virus titers in stocks were determined on Vero cells by limiting dilution assay for 50% tissue culture infectious doses ($TCID_{50}$s) by the method of Reed and Muench (50). The simian rotavirus SA-11 strain (ATCC) was propagated in MA-104 cells (European Collection of Cell Cultures [ECACC]) in MEM supplemented with 10% FCS, 1% L-glutamine, 1% nonessential amino acids, 50 μg/ml streptomycin, and 50 IU/ml penicillin.

Cell infection and follow-up. MTE cells were seeded at 250,000 cells per well on 24-well culture plates (Falcon) and incubated overnight at 37°C in a humidified atmosphere with 5% CO_2. The culture medium was then removed and cells were inoculated with 250 μl per well of CV-B4 E2 in DMEM at 5×10^2 $TCID_{50}$s/ml. In other experiments, MTE cell cultures (500,000 cells per well on 6-well culture plates [Falcon]) were inoculated with 3 ml per well of various virus suspensions (CV-B3, CV-B4 E2, CV-B4 JVB, E-1 Farouk, EMCV EMC, VSV, rotavirus SA-11, and HSV-1 HF) at 2.6×10^5 $TCID_{50}$s/ml. Mock-infected cells served as a negative control and were treated under the same conditions during all the experiments, except that they were inoculated with DMEM alone. At 1.30 h postinfection (p.i.), cells were washed with cold DMEM and then incubated with fresh culture medium. The medium was changed daily until day 8 p.i. and was then changed every 2 days. Cultures were examined daily under a light microscope, and at different time intervals p.i., one plate was stopped and processed as follows. Culture supernatants were removed, clarified, and stored at −80°C for CV-B4 E2 titration, performed on Vero cell monolayers by using the Reed-Muench method (50) (results are expressed as $TCID_{50}$s/ml), and for IGF-2 and IL-6 enzyme-linked immunosorbent assays (ELISAs). Cells were washed three times with cold DMEM and then prepared for RNA extraction, immunofluorescent (IF) staining, and viability assays.

SK-N-AS cells were seeded at 500,000 cells per well on 24-well culture plates (Falcon) and incubated overnight at 37°C in a humidified atmosphere with 5% CO_2. The culture medium was then removed and cells were inoculated with 250 μl per well of CV-B4 E2 in RPMI at different concentrations (2.1×10^2, 2.1×10^3, 2.1×10^4, 2.1×10^5, and 2.1×10^6 $TCID_{50}$s/ml). Cultures were then processed as described for MTE cells to study the effect of CV-B4 E2 infection on *Igf2* expression.

Metabolic activity of cells. Metabolic activity of MTE cells was estimated until day 43 p.i. 3-(4,5-Dimethyl-2-thiazolyl)-2,5-diphenyl-2H-tetrazolium bromide (MTT; Sigma) viable cell counting reagent, which identifies living cells through the formation of formazan complexes, was added to the washed cells. After 4 h of incubation at 37°C in a humidified atmosphere with 5% CO_2, the reaction was stopped by adding isopropanol–0.04 N HCl. The absorbance of the resulting formazan dye was measured on a spectrophotometer at wavelengths of 570 nm to 630 nm. Results are expressed as the percent viability compared to that for cells from mock-infected wells, for which viability was set to 100%.

The same protocol was used to follow and compare cellular multiplication for 1 week in both mock- and CV-B4 E2-inoculated MTE cultures during the chronic stage of the infection (in two separate experiments started at days 210 and 239 p.i., respectively). Results were expressed as the difference between the absorbance measured on a given day and that measured on the day at which the experiment was started (day 210 or day 239 p.i.), by seeding similar quantities of cells in each well of the culture plates to be processed.

IF staining. After careful washing, CV-B4 E2- and mock-infected MTE cells were processed as follows for immunostaining. Adherent cells were fixed and stained in culture plate wells to preserve their morphology, and floating cells were cytocentrifuged, fixed, and stained onto clean glass slides (10^5 cells per slide), following the same procedure. Briefly, cells were air dried and fixed in a solution of formaldehyde (reagent B; CMV Brite Turbo; IQ Products, Groningen, The Netherlands) for 5 min at room temperature. Cells were then washed for 3 min in phosphate-buffered saline (PBS) and permeabilized with Igepal Ca 630 detergent (reagent C; CMV Brite Turbo) for 1 min at room temperature. After a final wash of 3 min in PBS, preparations were stored at −80°C or processed immediately. Free aldehyde groups were reduced by incubating with a solution containing 50 mM NH_4Cl (Merck) and 20 mM glycine (Sigma) for 30 min at room temperature. After rinsing in Tris-buffered saline (TBS), preparations were processed to detect enterovirus VP1 peptide. Cells were stained by using the monoclonal mouse anti-enterovirus clone 5-D8/1 primary

TABLE 1 Oligonucleotide primers and probes[a]

Template	Prime type or probe	Nucleotide sequence[b]	Product size (bp)	Final concn	Reference
5′ noncoding region of CV-B4 RNA	Forward primer EV1	5′-CAAGCACTTCTGTTTCCCCGG-3′	435	0.4 μM	41
	Reverse primer EV2	5′-ATTGTCACCATAAGCAGCCA-3′	362		
	Internal reverse primer EV3	5′- CTTGCGCGTTACGAC-3′			
Human and mouse *Igf2* mRNA[c]	Forward primer	5′-ATGGGGAAGTCGATGCTGGTG-3′	316	0.4 μM	53
	Reverse primer	5′-ACGGGGTATCTGGGGAAGTTG-3′			
Mouse GAPDH	Forward primer	5′-AACGACCCCTTCATTGAC-3′	191	0.4 μM	55
	Reverse primer	5′-TCCACGACATACTCAGCAC-3′			
Human GAPDH	Forward primer	5′-GTCTTCACCACCATGGAGA-3′	206	0.4 μM	11
	Reverse primer	5′-CCAAAGTTGTCATGGATGACC-3′			
Mouse *Igf1* mRNA quantification	Forward primer	5′-CAGGCTATGGCTCCAGCATT-3′		200 nM	36
	Reverse primer	5′-ATAGAGCGGGCTGCTTTTG-3′		200 nM	
	Probe	5′-6-FAM-AGGGCACCTCAGACAGGCATTGTGG-BHQ-1-3′		200 nM	
Mouse *Igf2* mRNA quantification	Forward primer	5′-GGGAGCTTGTTGACACGCTT-3′		100 nM	36
	Reverse primer	5′-GCACTCTTCCACGATGCCA-3′		300 nM	
	Probe	5′-6-FAM-CAGGCCTTCAAGCCGTGCCAAC-BHQ-1-3′		200 nM	
Mouse *Ins2* mRNA quantification	Forward primer	5′-CCGGGAGCAGGTGACCTT-3′		150 nM	36
	Reverse primer	5′-GATCTACAATGCCACGCTTCTG-3′		150 nM	
	Probe	5′-6-FAM-AGACCTTGGCACTGGAGGTGGCC-BHQ-1-3′		100 nM	
Mouse HPRT mRNA quantification	Forward primer	5′-TTATCAGACTGAAGAGCTACTGTAATG-3′		300 nM	36
	Reverse primer	5′-CTTCAACAATCAAGACATTCTTTCC-3′		300 nM	
	Probe	5′-6-FAM-TGAGAGATCATCTCCACCAATAAC TTTTATGTCCC-BHQ-1-3′		100 nM	

[a] All primers used in qualitative RT-PCR were purchased from Sigma-Proligo. Primers and probes used for qPCRs were purchased from Eurogentec (Liège).
[b] FAM, 6-carboxyfluorescein; BHQ-1, black hole quencher dye 1.
[c] We have demonstrated that these primers, originally described for human *Igf2* mRNA (53), also recognize mouse *Igf2* mRNA.

antibody (Dako) for 2 h at 37°C. Following two washes in TBS, incubation with a fluorescein isothiocyanate (FITC)-conjugated rabbit anti-mouse immunoglobulin G (IgG; Argene SA) secondary antibody was performed for 1 h at 37°C. Evans blue (bioMérieux) incorporated with FITC, applied for 5 min just before mounting, was used for counterstaining to enumerate positive cells. After two washes in TBS, stained cells were reincubated with NH_4Cl-glycine solution for 10 min at room temperature. Preparations were then rinsed with TBS. For culture plates, 250 μl per well of TBS was added, and positive cells were directly enumerated under an inverted fluorescence microscope (Leitz Fluovert). Slides were mounted with Permafluor mounting medium (Coulter Immunotech), and positive cells were enumerated under a fluorescence microscope (Leitz Diaplan).

RNA extraction. Total RNA was extracted from a mixture of both adherent and floating MTE cells by the acid guanidium thiocyanate-phenol-chloroform extraction procedure by using Tri-Reagent (Sigma), as described by Chomczynski and Sacchi (11a). Extracted RNA was then dissolved in 50 μl of nuclease-free water (Promega), dosed with a Quant-iT RiboGreen RNA assay kit (Molecular Probes, Invitrogen) according to the manufacturer's instructions, and prepared to be used in reverse transcription (RT)-PCR assays. Purified water for injection (C.O.M Lavoisier) was submitted to the same extraction procedure and served as a negative control.

Removal of contaminating DNA from RNA extracts. The localization of both GAPDH (glyceraldehyde phosphate dehydrogenase) primers inside the same exon precludes the distinction between amplification products resulting from reverse-transcribed GAPDH mRNA and those arising from residual genomic DNA. For the expression of GAPDH mRNA serving as a standard to semiquantify *Igf2* mRNA expression, removal of residual genomic DNA from RNA extracts was essential. Thus, RNA samples were treated with RQ1 RNase-free DNase (Promega) for 30 min at 37°C, followed by inactivation at 65°C for 10 min, as recommended by the manufacturer. Samples were then immediately denatured at 90°C for 5 min and treated at 37°C for 30 min with recombinant exonuclease VII (USB), following the manufacturer's instructions, to ensure complete removal of contaminating DNA. After 10 min of inactivation at 95°C, samples were immediately put in ice and processed in RT-PCR assays. All reactions were performed by using a preheated Perkin Elmer Applied GeneAmp PCR system 2400.

Two-step RT-PCR for positive- and negative-strand CV-B4 E2 RNA detection. Either the sense (EV1) or the antisense (EV2) primer (Table 1) at 1 μM was used as the template in the synthesis of cDNA for negative- or positive-strand CV-B4 E2 RNA, respectively. The reaction was performed with about 60 to 70 ng of treated RNA in a total volume of 20 μl containing 20 U of Durascript reverse transcriptase, 0.5 mM each deoxynucleoside triphosphate (dNTP), 20 U of RNase inhibitor, 50 mM Tris-HCl (pH 8), 40 mM KCl, 8 mM $MgCl_2$, and 1 mM dithiothreitol by using a Durascript RT-PCR kit (Sigma) according to the manufacturer's instructions. Secondary structures were first denatured by heating the samples for 10 min at 80°C in the presence of dNTPs and the corresponding primer. The RT reaction was then performed at 50°C for 50 min, after

adding the reaction buffer, the enzyme, and the RNase inhibitor. The PCR was carried out with 5 μl of cDNA samples and 0.4 μM each primer in a total volume of 50 μl containing 2.5 U of JumpStart Accu *Taq* LA DNA polymerase, 0.2 mM each dNTP, 2.5 mM $MgCl_2$, 5 mM Tris-HCl, and 15 mM ammonium sulfate (pH 9.3). The PCR mixture was subjected to a first denaturation step for 2 min at 94°C, followed by 35 cycles of amplification, consisting of denaturation for 30 s at 94°C, annealing for 45 s at 55°C, and extension for 45 s at 68°C, followed by a final extension step for 7 min at 68°C. RNA extracted from CV-B4 E2-infected Vero cells was reverse transcribed, was amplified according to the procedure described above, and served as a positive control. A negative control (no RNA) was also included in each reaction. For all samples, GAPDH mRNA was amplified as described below and used as a positive control to demonstrate the absence of RT-PCR inhibitors. All reactions were performed by using a preheated Perkin Elmer Applied GeneAmp PCR system 2400.

Seminested RT-PCR for CV-B4 E2 applied directly on a few cells. A method for single PCR without extraction was described (43). That method was modified to detect viral RNA in a few cells. Briefly, cultured mock-infected and chronically CV-B4 E2-infected MTE cells, maintained in 6-well plates, were washed 10 times with cold PBS. Five hundred microliters of trypsin-EDTA (Eurobio) was then added in each well. After 5 to 7 min of incubation at 37°C, 2 ml per well of culture medium was added (to inhibit the trypsin), and the content of each well was recovered in 15-ml centrifugation tubes. After 5 min of centrifugation at 400 × *g* at 4°C, supernatants were removed and pellets were dissociated in 1 ml PBS. Cell suspensions were then enumerated with trypan blue and diluted to give approximately 10^5 cells/ml. Samples were then serially 2-fold diluted in PBS on 96-well microtiter plates, to obtain approximately 1 to 10 cells in the last wells. Plates were then centrifuged at 1,600 × *g* for 10 min, incubated at 65°C for 20 min, and immediately frozen at −80°C. Ten units of 10× Protector RNase inhibitor (Roche) per well was added immediately after thawing. cDNA synthesis and amplification were performed in a single tube by using a SuperScript One-Step RT-PCR with Platinum *Taq* kit (Invitrogen) according to the manufacturer's instructions. The reaction was performed in a total volume of 50 μl containing 10 μl of treated sample, 0.4 μM each EV1 and EV2 primers, 0.2 mM each dNTP, 1.2 mM $MgSO_4$, and 1 μl of reverse transcriptase enzyme-Platinum *Taq* mix. GAPDH primers (Table 1) were also included in the mix to ensure the presence of cells in each sample. Samples were subjected to a first step of reverse transcription for 30 min at 50°C, followed by 2 min of denaturation at 94°C; 40 cycles consisting of denaturation for 30 s at 94°C, annealing for 45 s at 55°C, and extension for 45 s at 72°C; and then a final extension step for 10 min at 72°C. RT-PCR products were then directly submitted to a seminested PCR by using the JumpStart AccuTaq LA DNA polymerase mix (Sigma) according to the manufacturer's instructions. The reaction was carried out with 5 μl of amplified DNA samples and 0.4 μM (each) primers EV1 and EV3 (Table 1) in a total volume of 50 μl containing 1 U of JumpStart Accu *Taq* LA DNA polymerase, 0.2 mM each dNTP, 2.5 mM $MgCl_2$, 5 mM Tris-HCl, 15 mM ammonium sulfate (pH 9.3), and 1% Tween 20. Samples were subjected to 3 min of denaturation at 94°C, followed by 35 cycles consisting of denaturation for 30 s at 94°C, annealing for 30 s at 52°C, and extension for 30 s at 72°C, followed by a final extension step for 7 min at 72°C. All reactions were performed by using a preheated Perkin Elmer Applied GeneAmp PCR system 2400.

One step RT-PCR for *Igf2* mRNA detection. cDNA synthesis and cDNA amplification were performed in a single tube by using the SuperScript One-Step RT-PCR with Platinum *Taq* kit as described above. Briefly, the reaction was performed with about 60 to 70 ng of treated RNA in the presence of 10 U Protector RNase inhibitor (for primers, see Table 1). Samples were subjected to a first step of reverse transcription for 30 min at 50°C, followed by 2 min of denaturation at 94°C; 40 cycles consisting of denaturation for 30 s at 94°C, annealing for 30 s at 55°C, and extension for 1 min at 72°C; and then a final extension step for 10 min at 72°C. Pooled RNA containing *Igf2* mRNA (QPCR human reference total RNA; Stratagene), together with pooled RNA extracted from fetal mouse thymus, was submitted to the same reaction and served as a positive control. For each RNA sample, GAPDH mRNA was amplified by the same method and used as a positive control to demonstrate the absence of RT-PCR inhibitors. A negative control (no RNA) was also included in each PCR. The removal of all contaminating genomic DNA was checked for each RNA sample by carrying out the GAPDH RT-PCR without the reverse transcription step. Only samples without contaminating genomic DNA have been considered. A negative control (no RNA) was included in each reaction. All reactions were performed by using a preheated Perkin Elmer Applied GeneAmp PCR system 2400.

Detection and analysis of amplification products. The amplified RT-PCR products were analyzed by electrophoresis on a 2% agarose gel containing 0.5 mg/ml ethidium bromide (Sigma) and visualized by using a Gel Doc 2000 system (Bio-Rad). A 100-bp DNA ladder (Invitrogen) was used as a molecular mass marker. Image processing and analysis operations of DNA bands were performed by using Quantity One software (Bio-Rad) as described previously (11). The relative quantities of *Igf2* and GAPDH RT-PCR products were compared by serial endpoint dilution. The results were expressed as the ratio of the absorbance of the *Igf2* amplicon to that of the GAPDH amplicon.

Quantitative RT-PCRs for *Igf1*, *Igf2*, and *Ins2*. Reverse transcription was performed using 250 ng of total RNA in a total volume of 20 μl by a Transcriptor first-strand cDNA synthesis kit (Roche) according to the manufacturer's instructions using an oligo(dT) primer. Reverse transcription products were used directly for quantitative PCRs (qPCRs) for *Igf1*, *Igf2*, type 2 insulin (*Ins2*; the insulin gene predominantly transcribed in the murine thymus), and the hypoxanthine-guanine phosphoribosyltransferase (HPRT) housekeeping gene, as previously described (36). One microliter of cDNA was added as a PCR template to 24 μl of a master mix containing iQ Supermix (Bio-Rad), the specific TaqMan probe, and primers (Table 1). Samples were subjected to a first step of activation of *Taq* polymerase for 2 min at 50°C, followed by 10 min of denaturation at 95°C and repeated cycles (40 for *Igf1*, *Ins2*, and HPRT and 45 for *Igf2*), with each one consisting of denaturation for 15 s at 95°C and a primer annealing/elongation step of 1 min at 60°C. Reactions were carried out on an iQ Cycler instrument (Bio-Rad). Every analysis contained a control tissue sample (the brain for *Igf2* and the liver for *Igf1*).

Calibration curves for *Igf1*, *Igf2*, *Ins2*, and HPRT were generated from serial dilutions of a specific cDNA plasmid (kindly provided by C. Mathieu, Legendo KUL, Belgium) for each gene. The range of calibration curves was from 10^7 to 10 molecules/μl. Results were calculated from the linear regression of the appropriate curve after real-time amplification.

ELISAs. Conditioned supernatants from mock- and CV-B4 E2-infected MTE cell cultures were collected at various times after inoculation and analyzed for murine IGF-2 and IL-6 proteins. Results, initially measured in pg/ml of culture supernatant, are expressed in relative amounts compared to those in mock-infected cultures, for which they were set to 100%.

To measure IGF-2, we used a mouse IGF-2 DuoSet ELISA development kit (R&D Systems) according to the manufacturer's instructions.

Murine IL-6 production in the culture supernatants was measured by a mouse IL-6 ELISA development kit (DuoSet; R&D Systems) according to the manufacturer's instructions.

Statistical analysis. Data are summarized as means ± standard deviations (SDs). The levels of various parameters in virus- and mock-infected cultures were compared using the Welch two-sample *t* test.

RESULTS

CV-B4 E2 infection of MTE cells. (i) Effects of CV-B4 E2 on MTE cell cultures. MTE cell cultures have been regularly observed by using an inverted microscope (Fig. 1A). In cultures inoculated with CV-B4 E2, small foci of rounded cells were observed as soon as day 2 p.i. Afterwards, that cytopathic effect (CPE) spread all over the culture, and a few cells detached from the cell layer by day 3 to day 5 p.i., until the majority became floating on day 5 to day 7

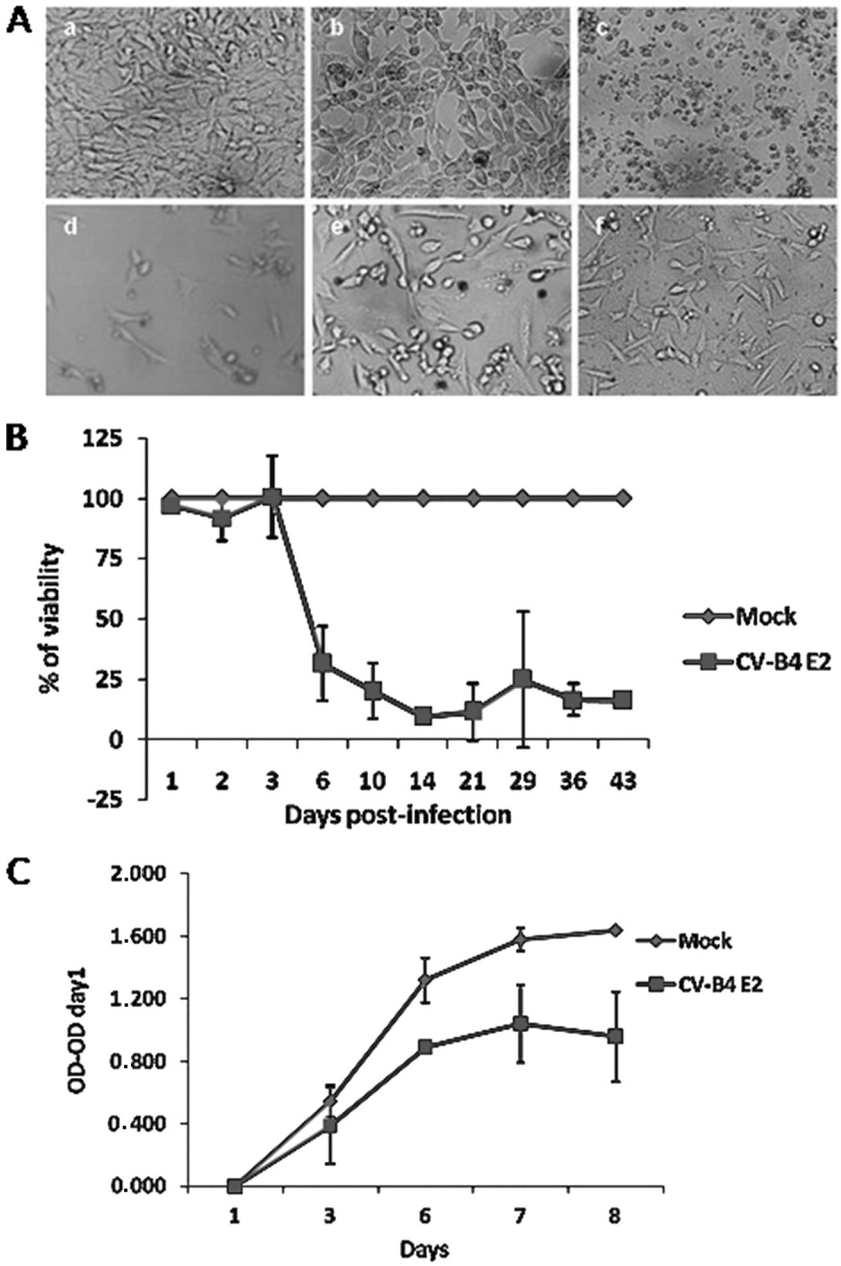

FIG 1 Effects of CV-B4 E2 on MTE cell cultures. (A) Effect of the virus on cell morphology and culture evolution. Microscopic observation of mock-infected (a) and CV-B4 E2-infected MTE cultures at 2 (b), 6 (c), 13 (d), 28 (e), and 56 (f) days p.i. Magnification, ×400. (B) Effect of the virus on cell viability by using the MTT metabolic activity test. Results are expressed as mean percentages of viability ± SDs in CV-B4 E2-infected cultures compared to mock-infected cultures, for which viability was set to 100% ($n = 3$). (C) Effect of the virus on cellular multiplication by using the MTT metabolic activity test in mock- and CV-B4 E2-infected MTE cultures for 1 week during the chronic stage of the infection. The tests were started with cells that were taken on day 210 or day 239 p.i. Results are expressed as means ± SDs of the difference between the absorbance measured on a given day (day 1 through 8) and the one measured when the experiment was started (optical density [OD] − optical density on day 1; $n = 2$; $P = 0.047$ versus mock-infected cultures).

p.i. Starting from day 8 to day 9 p.i., adherent as well as floating cells could be observed, and the cells continued regenerating and growing. There were rounded as well as intact cells, with wide fluctuations in the number of cells up to the end of the experiments. No evidence of a CPE was observed in mock-infected cultures all along the culture period.

Each time that the wells were overloaded in CV-B4 E2- or in mock-infected cultures, the cell layers disrupted, culture supernatants and floating cells were harvested, and then cells restarted growing. This occurred until the end of the follow-up.

The cell viability in CV-B4 E2-infected cultures compared to that in mock-infected cultures was assessed for 43 days p.i. by measuring the metabolic activity of cultures by using the MTT reagent. The metabolic activity was affected starting from day 6 in CV-B4 E2-infected cultures ($P < 0.001$ versus mock-infected cultures) (Fig. 1B). This was consistent with a significantly reduced

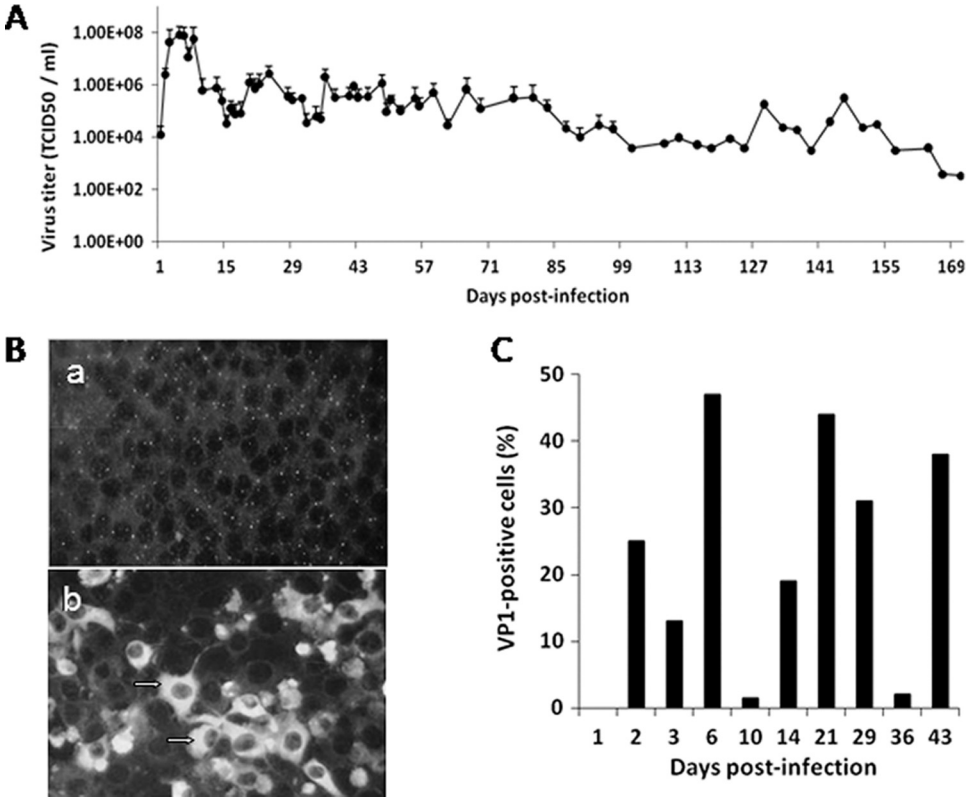

FIG 2 CV-B4 E2 replicates in MTE cells. (A) Titration of viral progenies in supernatants of CV-B4 E2-infected MTE cultures. Results are expressed as means of $TCID_{50}$s/ml + SDs ($n = 7$). (B) Indirect immunofluorescent staining for VP1 with FITC-conjugated antibodies and counterstaining with Evans blue of mock-infected (a) and CV- B4 E2-infected (b) cultures. Arrows, VP1-positive cells. Magnification, ×400. (C) Percentage of CV-B4 E2-infected MTE cells determined by detection of viral protein VP1 up to 43 days p.i. in a representative experiment out of 2.

mean number of cells in CV-B4 E2-infected cultures compared to mock-infected cultures (about 38,000 cells/well in CV-B4 E2-infected cultures versus 282,000 cells/well in mock-infected cultures on day 6 p.i., for example), which may explain the reduced metabolic activity obtained in our experiments. Cell viability and number in CV-B4 E2-infected cultures increased after the acute phase of the infection to become almost equivalent to those in mock-infected cultures during the chronic stage (data not shown). A similar pattern of results was observed in at least three independent experiments.

As described in the Materials and Methods section, cellular multiplication was also assessed with MTT reagent for 1 week during the chronic stage of the infection (in two separate experiments starting from day 210 and day 239 p.i., respectively). As shown in Fig. 1C, it is clear that CV-B4 E2-infected cells continued to grow and multiply to a lesser extent than cells in mock-infected cultures ($P = 0.047$ versus mock-infected cultures), but multiplication did not stop and was relatively well preserved.

(ii) CV-B4 E2 infection of MTE cells is productive. Infectious particles were released in culture supernatants of CV-B4 E2-infected MTE cells, as evidenced by titration on Vero cells (Fig. 2A). High titers of virus were found in the supernatants, peaking at between days 3 and 8 p.i. Then, viral titers were slightly lower but remained at relatively constant levels with moderate fluctuations until day 198 p.i., when the decrease became more pronounced (viral titers, between 10 and 100 $TCID_{50}$s/ml). Viral progeny was still detectable at 300 days p.i. (data not shown). Virus titration in supernatants of mock-infected cells was also performed, and no viral particles were detected in these samples (data not shown).

(iii) Viral protein VP1 can be detected by IF staining of CV-B4 E2-infected MTE cells. The viral protein VP1 has been detected by immunofluorescent staining (Fig. 2B and C), which allowed us to evaluate the proportion of infected cells in our experiments. Intracytoplasmic VP1 was detected as soon as day 2 p.i. through day 43 p.i. in CV-B4 E2-infected cultures (Fig. 2C) and was still detected at 200 days p.i. (data not shown). The proportion of VP1-positive cells showed wide fluctuations. Indeed, it peaked at 47%, 44%, and 43% at about days 6, 21, and 43 p.i., respectively, and decreased between these time points. Thereafter, the number of VP1-positive cells was reduced and remained at about 1 to 2% up to the end of the follow-up (data not shown). No VP1 staining could be evidenced in mock-infected cultures (Fig. 2Ba).

(iv) CV-B4 E2 RNA is detected in MTE cells. Intracellular positive- as well as negative-strand RNAs were detected starting from day 1 p.i. up to the end of the follow-up (day 300 p.i.) and further in CV-B4 E2-inoculated MTE cultures (Fig. 3A). CV-B4 positive- or negative-strand RNA was not detected in mock-infected cells (data not shown).

When cultures chronically infected with CV-B4 E2 were incubated in the presence of polyclonal rabbit anti-CV-B4 neutralizing antibody (100 neutralizing U/ml; kindly provided by J. J. Chomel, Centre National de Recherche sur les Entérovirus, Bron, France), viral RNA was not detectable in supernatants of cultures on day 14

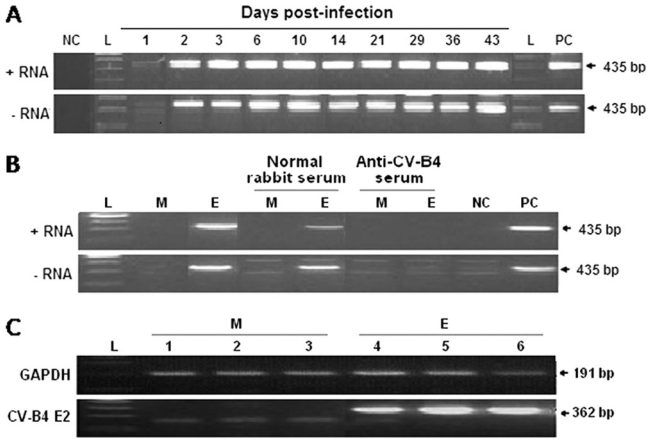

FIG 3 CV-B4 E2 RNA is detected in MTE cells. (A) Representative agarose gel electrophoresis of amplicons specific to the positive and negative strands of the CV-B4 E2 genome. Strand-specific RT-PCR was carried out on total RNA extracted from CV-B4 E2-infected MTE culture samples taken at different days p.i. Lanes L, 100-bp DNA molecular size ladder; lanes NC and PC, negative control (no RNA) and positive control (RNA extracted from CV-B4 E2-infected Vero cells), respectively. (B) Pattern of CV-BA E2 RNA in MTE cell cultures treated with rabbit serum. Strand-specific RT-PCR for CV-B4 E2 in mock-infected (lanes M) and CV-B4 E2-infected (lanes E) MTE culture samples taken before (at day 341 p.i.) and after (at day 400 p.i.) treatment (which started on day 351 p.i.) with either normal rabbit serum or rabbit anti-CV-B4 serum. (C) RT-PCR applied directly to a few cells. Representative agarose gel electrophoresis of amplicons specific to GAPDH (top) and CV-B4 E2 (bottom) mRNAs from a limited number of cells. Amplification was carried out on total lysates from 20 to 30 (lanes 1 and 4), 10 to 20 (lanes 2 and 5), and 1 to 10 (lanes 3 and 6) mock-infected (lanes M) and chronically CV-B4 E2-infected (lanes E) (210 days p.i.) MTE cells.

posttreatment (on day 351 p.i). Intracellular viral RNA was not detectable 29 days after that treatment (Fig. 3B). As expected, positive- and negative-strand CV-B4 E2 RNA remained unchanged when cultures were incubated in the presence of normal rabbit serum (Fig. 3B).

To investigate the extent of infection in MTE cell cultures in our experiments, cells taken at day 210 p.i. were thoroughly washed and serially diluted to obtain about 1 cell in the last tube. Then, the presence of enteroviral RNA in these cells was studied by RT-PCR without RNA extraction as described in the Material and Methods section. Viral RNA was detected in all tubes containing about 1 to 10 cells (Fig. 3C).

CV-B4 E2 infection and *Igf2* expression. (i) CV-B4 E2 infection results in a low level of *Igf2* mRNA in MTE cells. As shown in Fig. 4A, *Igf2* mRNA was detected in mock-infected MTE cell cultures, demonstrating that the MTE4-14 cell line spontaneously expresses *Igf2*, which enabled us to use this system for studying the impact of CV-B4 E2 infection on *Igf2* expression.

Igf2 transcripts were also detected in CV-B4 E2-infected MTE cell cultures (Fig. 4A). Equivalent expression of GAPDH housekeeping gene transcripts was observed in both mock- and CV-B4 E2-infected MTE cultures (Fig. 4A), which enabled us to use GAPDH mRNA as a standard to semiquantify *Igf2* mRNA. Figure 4B represents the percentages of *Igf2* transcripts in CV-B4 E2-infected cultures compared with mock-infected cultures, in which the level of *Igf2* transcripts was set to 100%. *Igf2* transcripts were first detected in CV-B4 E2-infected cells at levels comparable to those observed in mock-infected cultures until day 3, at which time they decreased slightly (between 84 and 90%) until day 14 p.i. and decreased markedly thereafter (between 52 and 60%). Then, after day 42 p.i., the levels of *Igf2* transcripts slightly increased but remained at levels significantly lower (between 61 and 74%) than those in mock-infected cultures until the end of the follow-up on day 300 p.i. and further ($P < 0.01$ versus mock-infected cultures).

To further investigate the effect of CV-B4 E2 infection on the expression of *Igf2*, we looked for another cell line that is able to produce *Igf2* and that can be infected with CV-B4 E2. We observed that CV-B4 E2 persistently infected neuroblastoma SK-N-AS cells, as attested to by the prolonged detection of positive- and negative-strand viral RNA (data not shown), but there was no effect on *Igf2* transcription in that system (Fig. 4C).

Real-time quantitative RT-PCR for *Igf2* confirmed the results of semiquantification (Fig. 4D). Indeed, experiments carried out on samples taken during the chronic stage of the infection (at 4 and 5 months p.i.) showed that the relative amounts of *Igf2* transcripts were drastically reduced in CV-B4 E2-infected MTE cells compared with mock-infected MTE cells (0.00026 versus 0.90986, respectively; $P < 0.01$). *Igf1* transcript levels were also decreased in CV-B4 E2-infected MTE cultures compared with mock-infected cultures (0.088 versus 4.699, respectively; $P < 0.05$), but to a lesser extent than *Igf2* transcripts (Fig. 4D). *Ins2* transcripts were absent or below the standard of the etalon curve of our quantitative real-time RT-PCR; they were not detected in either mock- or CV-B4 E2-infected MTE cultures (data not shown). The levels of the HPRT housekeeping gene were comparable in both mock- and CV-B4 E2-infected MTE cultures (data not shown).

(ii) CV-B4 E2 infection results in a low level of IGF-2 protein in MTE cell cultures. Figure 5A represents the relative amounts (percent) of IGF-2 protein measured by ELISA in supernatants of CV-B4 E2-infected MTE cell cultures compared with supernatants of mock-infected cultures, in which, due to wide fluctuations over time, the level of IGF-2 protein was set to 100%. IGF-2 protein was first detectable in CV-B4 E2-infected culture supernatants at levels comparable to those observed in mock-infected cultures and then at markedly decreased levels (below 20%) starting on day 6 p.i. (Fig. 5A). IGF-2 levels were significantly lower in CV-B4 E2-infected cell cultures than in mock-infected cultures ($P < 0.001$) up to the end of the follow-up on day 487 p.i.

The infection of MTE cells with UV-irradiated supernatants of MTE cultures chronically infected with CV-B4 E2 (taken on day 217 p.i.) had no significant effect on the concentration of IGF-2 protein compared with those in mock-infected cultures ($P = 0.087$; Fig. 5B).

In addition, the infection of MTE cells with UV-irradiated CV-B4 E2, concentrated beforehand by polyethylene glycol (PEG), had no effect on the IGF-2 concentration compared with that in mock-infected cultures ($P = 0.182$; Fig. 5C).

In order to investigate the effect of CV-B4 E2 infection on the expression of other proteins by MTE cells, we measured IL-6 expression by ELISA in the supernatants of mock- and CV-B4 E2-infected MTE cultures. As shown in Fig. 5D, in contrast to the level of IGF-2, the level of IL-6 in CV-B4 E2-infected cultures was significantly increased (mean, 429 pg/ml versus 111 pg/ml in mock-infected cultures; $P = 0.025$).

(iii) Effects of various viruses on IGF-2 protein expression by MTE cell cultures. Viruses had distinct effects on IGF-2 protein expression by MTE cells (Fig. 5E).

As observed in CV-B4 E2-infected MTE cell cultures, the IGF-2

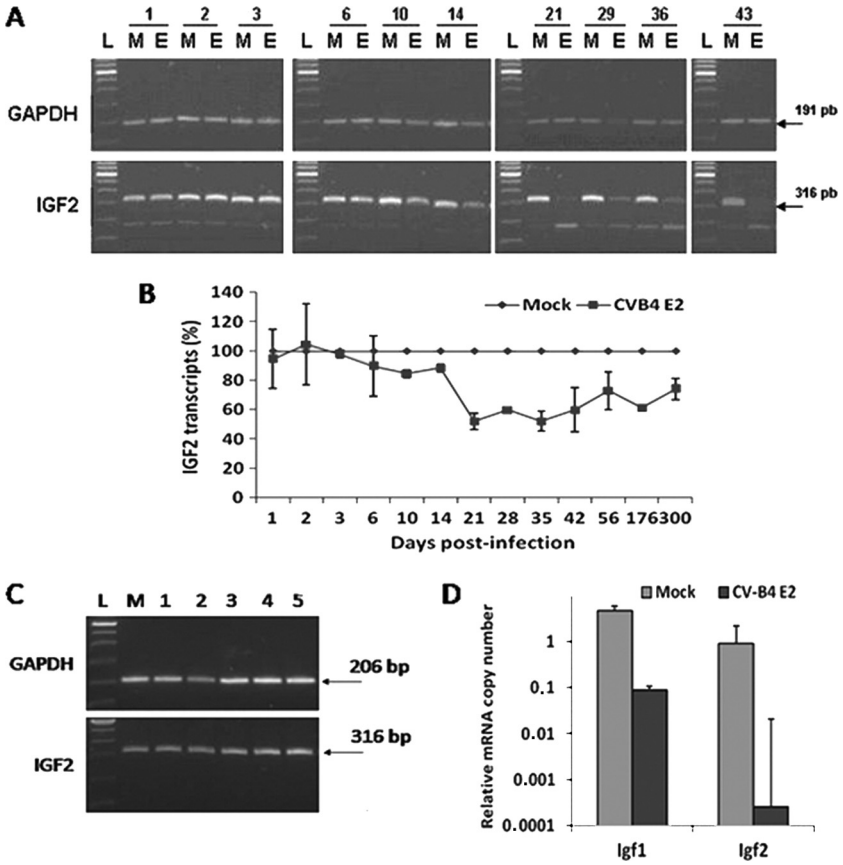

FIG 4 *Igf2* mRNA expression in MTE cultures. (A) Agarose gel electrophoresis of amplicons specific to the GAPDH (top) and *Igf2* (bottom) transcripts. RT-PCR was carried out on total RNA taken from mock-infected (lanes M) and CV-B4 E2-infected (lanes E) MTE cultures from 1 through 43 days p.i. Lanes L, 100-bp DNA molecular size ladder. Equivalent expression of GAPDH mRNA was detected in all samples. (B) Pattern of *Igf2* transcripts in MTE cultures. Semiquantification of *Igf2* mRNA expression in mock- and CV-B4 E2-infected MTE cells was performed by reference to the standard expression of GAPDH in those cells. The relative quantities of *Igf2* and GAPDH RT-PCR products were evaluated by serial endpoint dilution through the measurement of band absorbance. The means ± SDs of the ratio of the absorbance of the *Igf2* amplicon to that of the GAPDH amplicon were calculated, and the results were expressed as the percentage of the ratio value for the CV-B4 E2-infected culture relative to that for the mock-infected culture, for which the ratio value was set to 100% ($n = 4$, $P < 0.001$ versus mock-infected cells). (C) Effect of CV-B4 E2 on *Igf2* mRNA expression by SK-N-AS cells. Agarose gel electrophoresis of amplicons specific to the GAPDH (top) and *Igf2* (bottom) transcripts. RT-PCR was carried out on total RNA taken on day 63 p.i. from mock- and CV-B4 E2-infected SK-N-AS cultures. Lane M, mock-infected cultures; lanes 1 to 5, cultures infected with CV-B4 E2 at 2×10^8, 2×10^7, 2×10^6, 2×10^5, and 2×10^4 $TCID_{50}$s/ml, respectively. (D) Real-time quantification of *Igf1* and *Igf2* transcripts in mock- and CV-B4 E2-infected MTE cells was performed by reference to the expression of HPRT mRNA in those cells. Cells were harvested at 127 and 155 days p.i. Results are expressed as the mean ± SD of the *Igf1* or *Igf2* copy number after normalization with HPRT mRNA ($n = 4$; $P = 0.034$ versus mock-infected culture for *Igf1* and $P = 0.002$ versus mock-infected culture for *Igf2*).

concentration was markedly decreased in CV-B4 E2-, CV-B3-, CV-B4 JVB-, and echovirus 1 (E-1)-infected MTE cultures: means of 23 pg/ml (20%), 25 pg/ml (20%), 50 pg/ml (34%), and 47 pg/ml (36%) versus 140 pg/ml in mock-infected cultures (100%), respectively. These viruses persistently infected MTE cells, but without a CPE in the case of CV-B4 JVB and E-1 (data not shown). In contrast, the IGF-2 concentration markedly increased in HSV-1-infected MTE cultures (mean, 1,002 pg/ml; 842% versus mock-infected cultures), whereas rotavirus did not significantly disturb the expression of IGF-2 in that system (Fig. 5E). Rotavirus has no receptor on murine cells and, thus, could not infect MTE cells (data not shown). IGF-2 production could not be studied following EMCV or VSV infection, since both viruses induced the complete and rapid destruction of MTE cells (data not shown).

DISCUSSION

Thymic epithelial cells (TECs) play a critical role in the differentiation of T-cell precursors, providing a microenvironment with a unique capacity to generate functional and self-tolerant T cells (2, 3). Several viruses have been reported to infect human TECs (4, 48, 60). In this context, we have previously described the persistent infection of primary cultures of human TECs by CV-B4, and as a direct consequence, we have noted, interestingly, a modulation of cytokine production by those cells (5). However, with access to the human thymus being limited and maintenance of primary cultures being difficult, we chose to continue our investigations by using a cell line.

Selinka et al. (52) showed that 50-, 100-, and 120-kDa CV-B-binding proteins were present in mouse thymus, suggesting its permissiveness to CV-B infections. Indeed, CV-B4 infection of mouse thymus has already been reported *in vivo* (8, 27), as well as *in vitro* (6, 26). In the present work, it has been demonstrated that CV-B4 E2 can infect a murine TEC line of medullar origin, called MTE4-14 (42). The prolonged detection of both positive- and negative-strand viral RNA as well as VP1 protein in CV-B4 E2-inoculated cells clearly demonstrates that the MTE4-14 cell line

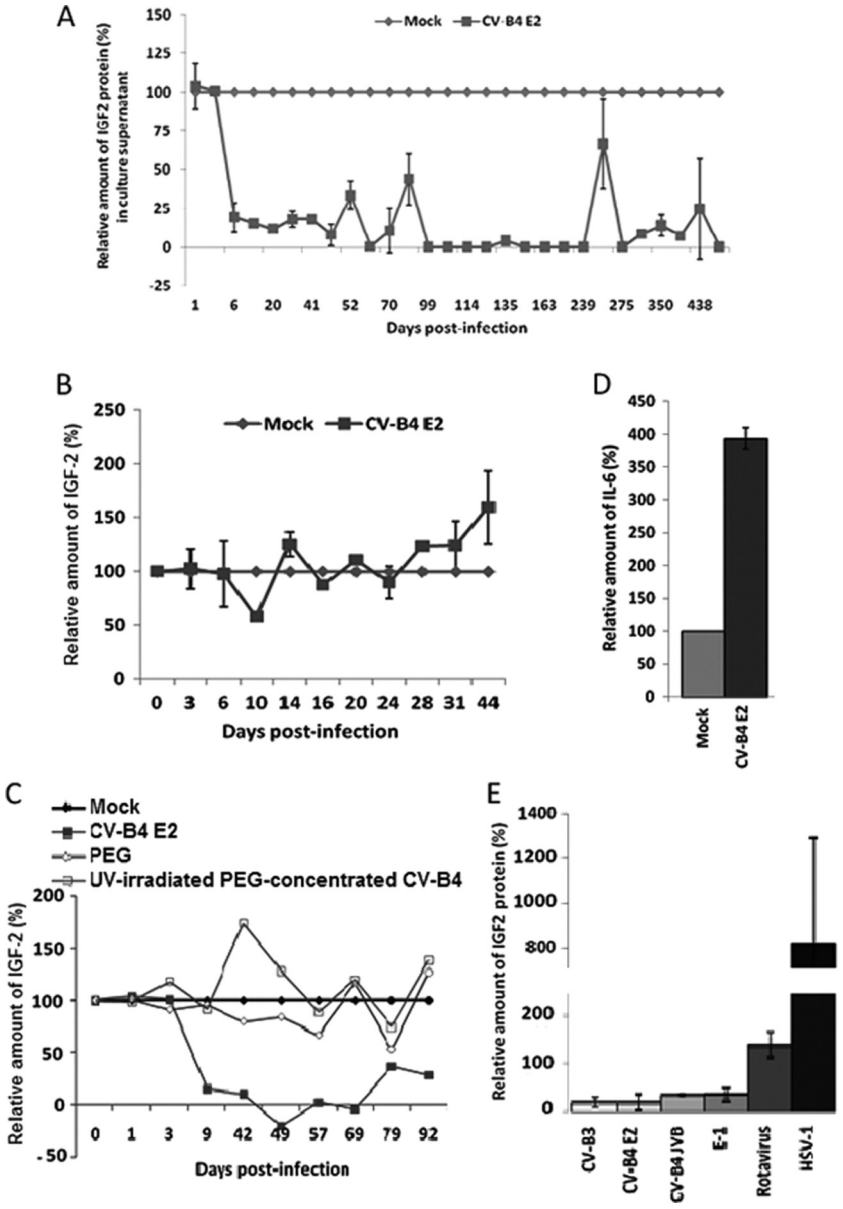

FIG 5 IGF-2 protein expression in MTE cell cultures. (A) Concentration of IGF-2 protein in supernatant of CV-B4 E2-infected MTE cell cultures measured by ELISA. The results are expressed as percentages compared with mock-infected cultures, in which the level of IGF-2 protein was set to 100% ($n = 2$; $P < 0.001$ versus mock-infected culture). (B) IGF-2 concentration in MTE cell cultures inoculated with UV-irradiated supernatants from mock-infected and chronically CV-B4 E2-infected MTE cultures (270 days p.i.). The levels of IGF-2 in supernatants were determined by ELISA and expressed as the mean percentages ± SDs in MTE cell cultures inoculated with UV-irradiated supernatant from CVB4 E2-infected MTE cell cultures (CV-B4 E2) compared to those inoculated with UV-irradiated supernatant from mock-infected MTE cell cultures (Mock), in which the level of IGF-2 protein was set to 100% ($P = 0.087$ versus mock-infected cultures; $n = 2$). (C) Pattern of IGF-2 concentration in supernatants of MTE cell cultures inoculated with PEG-concentrated CV-B4 E2. The IGF-2 concentration in supernatants of MTE cell cultures was determined by ELISA at different times p.i. Results from a representative experiment (out of two) are expressed as percentages compared to mock-infected cultures, in which the level of IGF-2 protein was set to 100%. (D) Effect of CV-B4 on the expression of IL-6 by MTE cells. IL-6 levels in supernatants of mock- and CV-B4 E2-infected MTE cells taken at days 127 and 156 p.i. were determined by ELISA. Results are expressed as mean percentages ± SDs compared to mock-infected cultures, in which the level of IL-6 protein was set to 100% ($n = 2$; $P = 0.025$ versus mock-infected cultures). (E) Profiles of IGF-2 concentration in supernatant of MTE cell cultures inoculated with various viruses. The levels of IGF-2 in supernatants taken at days 59 and 64 p.i. from mock-, CV-B3 Nancy-, CV-B4 E2-, CV-B4 JVB-, E-1 Farouk-, rotavirus SA-11-, and HSV-1 HF-infected MTE cells were determined by ELISA. Results are expressed as mean percentages ± SDs compared to mock-infected cultures, in which the level of IGF-2 protein was set to 100% ($n = 2$).

can sustain a persistent infection by this viral strain. This is consistent with previous reports on CV-B4 persistence in human pancreatic β cells (9, 63, 64), rhabdomyosarcoma (RD) cells (14), and human TECs (5). The results of PCR applied directly to a few cells suggest that an important proportion of TECs harbors enteroviral RNA during the chronic stage of the infection. The detection of viral progeny in culture supernatants indicates that the infection was productive, with virus replication and release occurring all along the follow-up. This is reminiscent of previous work in other systems, in which it has been observed that persistent infections

can be productive, with infectious virus continuously or intermittently detectable (5, 9, 45).

Previous reports clearly identified *Igf2* transcripts and immunoreactive IGF-2 protein within TECs of the subcapsular cortex and the medulla of human and rat thymus (17, 21, 34). In another investigation conducted on *Igf2*-transgenic mice, *Igf2* expression was shown to be restricted to the nonlymphocytic cells of the thymus (59). The basal expression of *Igf2* within the MTE4-14 cell line, as evidenced by the detection of its mRNA and protein in mock-infected cultures, gives an additional argument suggesting that *Igf2* is transcribed by medullary TECs. In addition, the MTE4-14 cell line that was derived from a neonatal thymus represents a suitable system to study *Igf2* expression, since it has previously been demonstrated that *Igf2* transcripts in mouse thymus decline a few days after birth (33).

IGF-2 is a single-chain polypeptide that shares amino acid sequence homology of about 47% with insulin and belongs to the insulin family of polypeptide growth factors. IGF-2 was shown to be the dominant polypeptide of the insulin family, being expressed in the thymus from different species. Thymic IGF-2 plays a dual role both in T-cell development and in T-cell negative selection (reviewed in reference 18). The intrathymic IGF-2-mediated cryptocrine signaling plays an active role in the early steps of T-cell differentiation during fetal development (33). Indeed, thymic IGF-2 exerts a role both in the early differentiation step from $CD4^-$ $CD8^-$ to $CD4^+$ $CD8^+$ cells and in determination of differentiation into the CD4 or CD8 lineage, since anti-IGF-2 antibody treatment induced a significant increase in the frequency of $CD4^-$ $CD8^-$ and $CD4^-$ $CD8^+$ cells, together with a decrease in $CD4^+$ $CD8^+$ cells in murine fetal thymic organ cultures. On the other hand, IGF-2 or IGF-2-derived self-antigen presentation in the thymic microenvironment might play a role in the induction of central tolerance toward the insulin family and islet β cells (reviewed in references 18 and 20). Moreover, it has been demonstrated that $Igf2^{-/-}$ mice are significantly less tolerant to insulin than wild-type mice (23).

We took advantage of *Igf2* expression by MTE cells to study the possible impact of CV-B4 E2 infection on the synthesis of that important protein potentially involved in the immune tolerance toward the whole insulin hormone family. In the current study, we showed that CV-B4 E2 infection of MTE cells was followed by significantly reduced amounts of *Igf2* transcripts and IGF-2 protein.

The decrease in the relative amounts of *Igf2* transcripts and IGF-2 protein in MTE cell cultures was not an exclusive effect of CV-B4 E2 since a similar effect was obtained in MTE cell cultures infected with the prototype strains CV-B4 JVB, CV-B3 Nancy, and E-1 Farouk, all belonging to the type B human enterovirus (HEV-B) species. The impairment in *Igf2* transcription and IGF-2 production was observed a few days after the infection and persisted up to the end of the follow-up. That effect was not a result of cell lysis, since CV-B4 E2-infected MTE cells were growing and living, as evidenced by viability test results, and since it was observed in CV-B4 JVB- and E-1 Farouk-infected cultures, in which there was no evident CPE. Altogether, these data suggest that *Igf2* (and, to a lesser extent, *Igf1*) transcription is selectively impaired within the remaining viable cells.

The inoculation of MTE cells with UV-irradiated supernatants from CV-B4 E2-infected Vero cultures (data not shown) or from chronically infected MTE cultures had no consequence on *Igf2* expression, which excludes the possibility of a role for soluble factors contained in these supernatants and strengthens the hypothesis of the direct role of the virus. Viral proteins were not implicated, since the incubation of MTE cell cultures in the presence of UV-irradiated CV-B4, concentrated beforehand by PEG, did not impair *Igf2* expression.

During the chronic stage of the infection, the proportion of VP1-positive cells was only 1 to 2% in MTE cell cultures, whereas the IGF-2 concentration was maintained at a significantly lower level compared to that in mock-infected cultures. Altogether, these data suggest that the impairment of *Igf2* transcription may be linked to the presence of CV-B4 E2 RNA in cells. This hypothesis is supported by the prolonged detection of viral RNA (at 210 days p.i. and further) even when focusing on a very few cells, suggesting that a large proportion of cells was infected during the chronic stage of the infection and better explaining the prolonged drastic effect on *Igf2* expression. This effect does not depend on type 3 Toll-like receptor (TLR3), which recognizes double-stranded viral RNA replication intermediates, since poly(I · C) did not decrease *Igf2* expression in MTE cultures (data not shown). The last observation rather suggests the involvement of single-stranded RNA or of other viral RNA sensors in the impairment of *Igf2* expression in CV-B4 E2-infected MTE cell cultures.

The current results show that the MTE4-14 cell line is a suitable system to study the effect of viruses on *Igf2* expression and are reminiscent of those obtained by other authors in various models. Indeed, it has been reported that viruses that establish persistent infections may have selective effects on the host's transcriptional machinery (37). It has been shown that in a rat pituitary cell line infected with lymphocytic choriomeningitis virus (LCMV), the virus markedly interfered with growth hormone (GH) but only minimally interfered with the expression of other genes (13). Altogether, our data and those reported by other teams show that a virus can disrupt the synthesis of a cell product without perturbing the vital cellular functions.

This is the first investigation of the effect of viruses on *Igf2* expression in thymic cells. Indeed, in previous studies, it was shown that the *Igf2* pathway can be affected by virus infections in other systems, such as chronic hepatitis B virus (HBV) or hepatitis C virus (HCV) infection in human liver cells (25, 39, 40) and alphaherpesviruses in primary rat embryonic fibroblasts (49). In those reports, virus infections were followed by activation of *Igf2* expression, which was observed in HSV-1-infected MTE cell cultures in our experiments. Together the present results and those of other groups suggest that *Igf2* can be the target of virus-induced activation or impairment.

A defect in thymic *Igf2* expression has been discovered in BBDP rats and correlated with the emergence of autoimmune diabetes in these animals. It has been suggested that the defect in thymic IGF-2 in those rats contributes to the absence of central T-cell self-tolerance toward members of the insulin family (by defective negative selection of self-reactive T cells), which resulted in the onset of the disease (32). Previous studies showed that a defect in thymic *Igf2* expression can be induced by genetic mutations, such as in the BBDP rat model. The present study shows that an impairment of *Igf2* expression in TECs can be induced by viruses such as HEV-Bs (CV-B3, CV-B4 E2 and JVB, and E-1 Farouk). CV-B4 E2 infection of the neuroblastoma cell-line SK-N-AS had no effect on *Igf2* expression, contrasting with data ob-

tained in the thymic cell line, which indicates that the viral effect on *Igf2* depends on the host cell.

Insofar as all ubiquitous and tissue-specific genes are expressed within the thymic medulla, the medullar MTE4-14 cell line opens the possibility of studying the effect of viruses on the expression of various genes potentially involved in establishment of self-tolerance toward islet β cells. *Ins2* was not expressed by MTE cells or was expressed at a very low level below the detection threshold of our RT-qPCR. The latter observation is not so surprising, since a very low degree of insulin gene transcription in healthy murine and human thymus had already been described and correlated to the poor tolerogenicity of insulin protein evidenced in many studies (20). In contrast, *Igf1* transcripts were detectable, and a decreased level of these transcripts was observed in CV-B4 E2-infected MTE cultures as well, but to a lesser extent than *Igf2* transcripts. IGF-1 acts as a positive thymic regulator by stimulating thymus growth and thymopoiesis (12, 33). Indeed, it has been observed that age-related declines in thymic function paralleled declines in plasma concentrations of IGF-1 (35). In murine fetal thymic organ cultures, inhibition of IGF-1 by antibody blockade resulted in significant changes in total thymocyte numbers and subset composition (33). Administration of exogenous IGF-1 to genetically altered mice demonstrated that the predominant effect of IGF-1 on thymic function is through its effects on TEC numbers and function, which in turn supports enhanced T-cell development (12). With regard to tolerogenicity, IGF-1 is less tolerogenic than IGF-2, which can be explained by a hierarchically higher thymic expression of *Igf2* (16).

Clearly, the low IGF-2 concentration in CV-B4 E2-infected MTE cell cultures was not the consequence of global cell impairment, since high levels of IL-6 were measured. While many changes in the biology of infected cells may result directly from the inhibition of cellular translation, it is also true that several preexisting proteins in the infected cell are specifically targeted during viral infection. Indeed, in a previous investigation, two-dimensional gel electrophoresis of [^{35}S]methionine-labeled HeLa cell proteins revealed that although most proteins were unaffected during the course of poliovirus infection, 10 to 14 different cellular proteins were missing in the infected samples (58).

In conclusion, the current investigation provides for the first time a description of the infection of a thymic epithelial cell line by enteroviruses. A persistent infection of that cell line with CV-B4 E2 was obtained and was accompanied by a reduced level of *Igf2* (and, to a lesser extent, of *Igf1*) transcription. Together these data suggest that CV-B4 E2 infection of the thymus may affect the expression of genes that can play a role in the tolerance toward islet β cells. Other studies are needed to investigate further the mechanism of the disturbed *Igf2* expression in this system.

ACKNOWLEDGMENTS

We thank F. Trottein (Centre d'Infection et d'Immunité de Lille, CNRS, Insitut Pasteur Lille) for IL-6 measurements.

This work was supported by the Ministère de l'Education Nationale de la Recherche et de la Technologie, Université Lille 2 (UPRES EA3610), France, and CHRU Lille and by the EU FP6 Integrated Project EUROTHYMAIDE (contract LSHB-CT-2003-503410). Additionally, part of the study was funded by EU FP7 (GA-261441-PEVNET). This work was also supported by the Ministère de la Recherche Scientifique, de la Technologie et du Développement des Compétences (LR99-ES27), Tunisia. Hela Jaïdane was supported by the Comité Mixte de Coopération Universitaire (CMCU 04/G0810) with grants from Egide Paris.

REFERENCES

1. **Anderson MS, et al.** 2002. Projection of an immunological self shadow within the thymus by the aire protein. Science **298**:1395–1401.
2. **Bonomo A, Matzinger P.** 1993. Thymus epithelium induces tissue-specific tolerance. J. Exp. Med. **177**:1153–1164.
3. **Boyd RL, et al.** 1993. The thymic microenvironment. Immunol. Today **14**:445–459.
4. **Braun J, et al.** 1996. Productive and persistent infection of human thymic epithelial cells in vitro with HIV-1. Virology **225**:413–418.
5. **Brilot F, et al.** 2002. Persistent infection of human thymic epithelial cells by coxsackievirus B4. J. Virol. **76**:5260–5265.
6. **Brilot F, Geenen V, Hober D, Stoddart CA.** 2004. Coxsackievirus B4 infection of human fetal thymus cells. J. Virol. **78**:9854–9861.
7. **Brilot F, Jaïdane H, Geenen V, Hober D.** 2008. Coxsackievirus B4 infection of murine foetal thymus organ cultures. J. Med. Virol. **80**:659–666.
8. **Chatterjee NK, Hou J, Dockstader P, Charbonneau T.** 1992. Coxsackievirus B4 infection alters thymic, splenic, and peripheral lymphocyte repertoire preceding onset of hyperglycemia in mice. J. Med. Virol. **38**:7124–7131.
9. **Chehadeh W, et al.** 2000. Persistent infection of human pancreatic islets by coxsackievirus B is associated with alpha interferon synthesis in beta cells. J. Virol. **74**:10153–10164.
10. **Chehadeh W, et al.** 2000. Increased level of interferon-alpha in blood of patients with insulin-dependent diabetes mellitus: relationship with coxsackievirus B infection. J. Infect. Dis. **181**:1929–1939.
11. **Chehadeh W, Bouzidi A, Alm G, Wattre P, Hober D.** 2001. Human antibodies isolated from plasma by affinity chromatography increase the coxsackievirus B4-induced synthesis of interferon-alpha by human peripheral blood mononuclear cells in vitro. J. Gen. Virol. **82**:1899–1907.

11a. **Chomczynski P, Sacchi N.** 1987. Single-step method of RNA isolation by acid guanidinium thiocyanate-phenol-chloroform extraction. Anal. Biochem. **162**:156–159.

12. **Chu YW, et al.** 2008. Exogenous insulin-like growth factor 1 enhances thymopoiesis predominantly through thymic epithelial cell expansion. Blood **112**:2836–2846.
13. **de la Torre JC, Oldstone MBA.** 1992. Selective disruption of growth hormone transcription machinery by viral infection. Proc. Natl. Acad. Sci. U. S. A. **89**:9939–9943.
14. **Frisk G, Lindberg MA, Diderholm H.** 1999. Persistence of coxsackievirus B4 infection in rhabdomyosarcoma cells for 30 months. Brief report. Arch. Virol. **144**:2239–2245.
15. **Gamble DR, Taylor KW, Cumming H.** 1973. Coxsackie viruses and diabetes mellitus. Br. Med. J. **4**:260–262.
16. **Geenen V.** 2003. The thymic insulin-like growth factor axis: involvement in physiology and disease. Horm. Metab. Res. **35**:656–663.
17. **Geenen V, et al.** 1993. Evidence that insulin-like growth factor II (IGF-II) is the dominant member of the insulin superfamily. Thymus **21**:115–127.
18. **Geenen V, Lefèbvre PJ.** 1998. The intrathymic expression of insulin-related genes: implications for pathophysiology and prevention of type 1 diabetes. Diabetes Metab. Rev. **14**:95–103.
19. **Geenen V, Louis C, Martens H.** 2004. An insulin-like growth factor 2-derived self-antigen inducing a regulatory cytokine profile after presentation to peripheral blood mononuclear cells from DQ8+ type 1 diabetic adolescents: preliminary design of a thymus-based tolerogenic self-vaccination. Ann. N. Y. Acad. Sci. **1037**:59–64.
20. **Geenen V, et al.** 2010. Thymic self-antigens for the design of a negative/tolerogenic self-vaccination against type 1 diabetes. Curr. Opin. Pharmacol. **10**:461–472.
21. **Han VKM, D'Ercole AJ, Lund PK.** 1987. Cellular localization of somatomedin (IGF) messenger RNA in the human fetus. Science **236**:193–197.
22. **Han VKM, Lund PK, Lee DC, D'Ercole AJ.** 1988. Expression of somatomedin/insulin-like growth factor messenger ribonucleic acids in the human fetus: identification, characterization, and tissue distribution. J. Clin. Endocrinol. Metab. **66**:422–429.
23. **Hansenne I, Renard-Charlet C, Greimers R, Geenen V.** 2006. Dendritic cell differentiation and tolerance to insulin-related peptides in *Igf2*-deficient mice. J. Immunol. **176**:4651–4657.
24. **Hober D, Sauter P.** 2010. Pathogenesis of type 1 diabetes mellitus: interplay between enterovirus and host. Nat. Rev. Endocrinol. **6**:279–289.
25. **Iizuka N, et al.** 2002. Comparison of gene expression profiles between hepatitis B virus- and hepatitis C virus-infected hepatocellular carcinoma

by oligonucleotide microarray data on the basis of a supervised learning method. Cancer Res. **62**:3939–3944.
26. **Jaïdane H, et al.** 2008. Infection of primary cultures of murine splenic and thymic cells with coxsackievirus B4. Microbiol. Immunol. **52**:40–46.
27. **Jaïdane H, et al.** 2006. Prolonged viral RNA detection in blood and lymphoid tissues from coxsackievirus B4E2 orally-inoculated Swiss mice. Microbiol. Immunol. **50**:971–974.
28. **Jaïdane H, Hober D.** 2008. Role of coxsackievirus B4 in the pathogenesis of type 1 diabetes. Diabetes Metab. **34**:537–548.
29. **Jaïdane H, et al.** 2012. Immunology in the clinic review series; focus on type 1 diabetes and viruses: enterovirus, thymus and type 1 diabetes pathogenesis. Clin. Exp. Immunol. **168**:39–46.
30. **Jaïdane H, et al.** 2010. Enteroviruses and type 1 diabetes: towards a better understanding of the relationship. Rev. Med. Virol. **20**:265–280.
31. **Kappler JW, Roehm N, Marrack P.** 1987. T cell tolerance by clonal elimination in the thymus. Cell **49**:273–280.
32. **Kecha-Kamoun O, et al.** 2001. Thymic expression of insulin-related genes in an animal model of autoimmune type 1 diabetes. Diabetes Metab. Res. Rev. **17**:146–152.
33. **Kecha O, et al.** 2000. Involvement of insulin-like growth factors in early T cell development: a study using fetal thymic organ cultures. Endocrinology **141**:1209–1217.
34. **Kecha O, et al.** 1999. Characterization of the insulin-like growth factor axis in the human thymus. J. Neuroendocrinol. **11**:435–440.
35. **Kelley KW, et al.** 1998. Insulin growth factor-I inhibits apoptosis in hematopoietic progenitor cells: implications in thymic aging. Ann. N. Y. Acad. Sci. **840**:518–524.
36. **Kermani H, et al.** 2012. Expression of the growth hormone/insulin-like growth factor axis during Balb/c thymus ontogeny and effects of growth hormone upon ex vivo T cell differentiation. Neuroimmunomodulation **19**:137–147.
37. **Klavinskis LS, Oldstone MB.** 1989. Lymphocytic choriomeningitis virus selectively alters differentiated but not housekeeping functions: block in expression of growth hormone gene is at the level of transcriptional initiation. Virology **168**:232–235.
38. **Klein L, Kyewski B.** 2000. "Promiscuous" expression of tissue antigens in the thymus: a key to T-cell tolerance and autoimmunity? J. Mol. Med. **78**:483–494.
39. **Lee YI, et al.** 1998. The human hepatitis B virus transactivator X gene product regulates Sp1 mediated transcription of an insulin-like growth factor II promoter 4. Oncogene **16**:2367–2380.
40. **Lee S, Park U, Lee YI.** 2001. Hepatitis C virus core protein transactivates insulin-like growth factor II gene transcription through acting concurrently on Egr1 and Sp1 sites. Virology **283**:167–177.
41. **Leparc I, Aymard M, Fuchs F.** 1994. Acute, chronic and persistent enterovirus and poliovirus infections: detection of viral genome by semi-nested PCR amplification in culture-negative samples. Mol. Cell. Probes **8**:487–495.
42. **Lepesant H, Pierres M, Naquet P.** 1995. Deficient antigen presentation by thymic epithelial cells reveals differential induction of T cell clone effector functions by CD28-mediated costimulation. Cell. Immunol. **161**: 279–287.
43. **Li HH, et al.** 1988. Amplification and analysis of DNA sequences in single human sperm and diploid cells. Nature **335**:414–417.
44. **Maha MM, et al.** 2003. The role of coxsackieviruses infection in the children of insulin dependent diabetes mellitus. J. Egypt. Public Health Assoc. **78**:305–318.
45. **Miller JR.** 1981. Prolonged intracerebral infection with poliovirus in asymptomatic mice. Ann. Neurol. **9**:590–596.
46. **Moya-Suri V, et al.** 2005. Enterovirus RNA sequences in sera of school-children in the general population and their association with type 1-diabetes-associated autoantibodies. J. Med. Microbiol. **54**:879–883.
47. **Nairn C, Galbraith DN, Taylor KW, Clements GB.** 1999. Enterovirus variants in the serum of children at the onset of type 1 diabetes mellitus. Diabet. Med. **16**:509–513.
48. **Numazaki K, Goldman H, Bai XQ, Wong I, Wainberg MA.** 1989. Effects of infection by HIV-1, cytomegalovirus, and human measles virus on cultured human thymic epithelial cells. Microbiol. Immunol. **33**:733–745.
49. **Ray N, Enquist LW.** 2004. Transcriptional response of a common permissive cell type to infection by two diverse alphaherpesviruses. J. Virol. **78**:3489–3501.
50. **Reed LJ, Muench H.** 1938. A simple method of estimating fifty percent endpoints. Am. J. Hyg. **27**:493–497.
51. **Seddon B, Mason D.** 2000. The third function of the thymus. Immunol. Today **21**:95–99.
52. **Selinka HC, et al.** 1998. Coxsackie B virus and its interaction with permissive host cells. Clin. Diagn. Virol. **9**:115–123.
53. **Shaddy RE, Zhang YL, White WL.** 1996. Murine and pediatric myocardial growth factor mRNA using reverse transcription-polymerase chain reaction. Biochem. Mol. Med. **57**:10–13.
54. **Shevach EM.** 2000. Regulatory T cells in autoimmunity. Annu. Rev. Immunol. **18**:423–449.
55. **Simpson DAC, Feeney S, Boyle C, Stitt AW.** 2000. Retinal VEGF mRNA measured by SYBR green I fluorescence: a versatile approach to quantitative PCR. Mol. Vis. **6**:178–183.
56. **Sinha AA, Lopez MT, McDevitt HO.** 1990. Autoimmune diseases: the failure of self tolerance. Science **248**:1380–1388.
57. **Sugimoto T, et al.** 1984. Determination of cell surface membrane antigens common to both human neuroblastoma and leukemia-lymphoma cell lines by a panel of 38 monoclonal antibodies. J. Natl. Cancer Inst. **73**:51–57.
58. **Urzainqui A, Carrasco L.** 1989. Degradation of cellular proteins during poliovirus infection: studies by two-dimensional gel electrophoresis. J. Virol. **63**:4729–4735.
59. **Van der Ven LT, Roholl PJ, Reijnen-Gresnigt MG, Bloemen RJ, van Buul-Offers SC.** 1997. Expression of insulin-like growth factor II (IGFII) and histological changes in the thymus and spleen of transgenic mice overexpressing IGF-II. Histochem. Cell Biol. **107**:193–203.
60. **Wainberg MA, Numazaki K, Destephano L, Wong I, Goldman H.** 1988. Infection of human thymic epithelial cells by human cytomegalovirus and other viruses: effect on secretion of interleukin 1-like activity. Clin. Exp. Immunol. **72**:415–421.
61. **Yang Y, Guo L, Ma L, Liu X.** 1999. Expression of growth hormone and insulin-like growth factor in the immune system of children. Horm. Metab. Res. **31**:380–384.
62. **Yeung WC, Rawlinson WD, Craig ME.** 2011. Enterovirus infection and type 1 diabetes mellitus: systematic review and meta-analysis of observational molecular studies. BMJ **342**:d35. doi:10.1136/bmj.d35.
63. **Yin H, Berg AK, Westman J, Hellerstrom C, Frisk G.** 2002. Complete nucleotide sequence of a coxsackievirus B-4 strain capable of establishing persistent infection in human pancreatic islet cells: effects on insulin release, proinsulin synthesis, and cell morphology. J. Med. Virol. **68**:544–557.
64. **Yoon JW, Onodera T, Jenson AB, Notkins AL.** 1978. Virus induced diabetes mellitus XI. Replication of coxsackie B3 in human pancreatic beta cell cultures. Diabetes **27**:778–781.
65. **Yoon JW, Austin M, Onodera T, Notkins AL.** 1979. Isolation of a virus from the pancreas of a child with diabetic ketoacidosis (virus-induced diabetes mellitus). N. Engl. J. Med. **300**:1173–1179.